# Hysteretic ac losses and susceptibility of thin superconducting disks

John R. Clem
*Ames Laboratory–U.S. Department of Energy and Department of Physics, Iowa State University, Ames, Iowa 50011*

Alvaro Sanchez
*Departament de Física, Universitat Autònoma de Barcelona, 08193 Bellaterra, Barcelona, Spain*
(Received 20 June 1994)

We calculate hysteretic magnetization curves and ac-susceptibility components $\chi_n'$ and $\chi_n''$ for $n=1$, 3, and 5 for a type-II superconducting thin circular disk subjected to a low-frequency oscillating applied field, extending previous approaches for calculating hysteretic current-density and magnetic flux-density profiles in the critical state. We also present limiting expressions for $\chi'=\chi_1'$ and $\chi''=\chi_1''$ for both small and large values of the ac field amplitude, and we show how $\chi''$ is simply related to the ac loss per cycle per unit volume. Finally, a comparison is made between our results and those obtained for slab and strip geometries.

## I. INTRODUCTION

Recently there has been much interest in the properties of superconducting films in time-varying applied magnetic fields. Such properties are of importance for both fundamental and applied reasons. For example, superconductors have considerable potential for use in specialized electronics applications, and it is important to know how magnetic flux penetrates thin-film superconductors and how large the corresponding ac losses are.

A critical-state theory for the penetration of magnetic flux into thin type-II superconducting strips of infinite length was developed in 1970 by Norris,[1] and several recent papers[2,3] have applied this approach to study more complicated problems in strip geometry.

An important theoretical advance recently has been made by Mikheenko and Kuzovlev,[4] who showed how to apply the critical-state theory to thin superconducting disks. This work has been extended (and corrected) by Zhu *et al.*[5] The latter paper contains the basic information that is needed to calculate the hysteretic ac losses in a thin superconducting disk, as well as related properties such as the complex ac susceptibility.

In the present paper, we begin in Sec. II by briefly reviewing what is known about the distribution of currents in a thin superconducting disk in the presence of a perpendicular applied field. We first discuss the behavior in very small applied fields, where no vortices penetrate but induced supercurrents flow in circular patterns around the axis of the disk. We then treat the behavior in the critical state, where vortices penetrate the disk edges. The magnitude of the current density $\mathbf{J}$ in the flux-penetrated annulus is $J_c$, the critical-current density, while in the nonpenetrated region inside this annulus the magnitude of $\mathbf{J}$ is less than $J_c$ but is not zero, except on the axis. The latter behavior contrasts strongly with that in an infinitely long superconducting cylinder.

In Sec. III, we show calculations of the disk's magnetic moment in a low-frequency oscillating applied magnetic field, and display results for the magnetization hysteresis loops. In Sec. IV, we extend the results of Ref. 5 by Fourier analyzing the magnetization in terms of the ac susceptibility coefficients $\chi_n'$ and $\chi_n''$ and by presenting a general result relating the ac loss per cycle to the $n=1$ component of the imaginary part, $\chi''=\chi_1''$. In Sec. V, we apply these results to calculate and display $\chi_n'$ and $\chi_n''$ (for $n=1$, 3, and 5) as universal functions when the Bean model [$J_c(B)=$const] applies.[6] Finally, in Sec. VI, we summarize our results and relate them to other work in this field.

## II. CURRENT-DENSITY AND MAGNETIC-FIELD PROFILES IN A THIN SUPERCONDUCTING DISK

In this paper we consider a high-$\kappa$ type-II superconducting disk of radius $R$ and uniform thickness $d$, where $d \ll R$. We assume either that $d \geq \lambda$, where $\lambda$ is the London penetration depth, or, if $d < \lambda$, that $\Lambda = 2\lambda^2/d \ll R$, where $\Lambda$ is the two-dimensional screening length.[7,8] (The approach given in the present paper would require further extensions to handle the weak-screening limit for which $\Lambda \geq R$.) We suppose that the disk is in the $x$-$y$ plane, centered on the $z$ axis, and we use cylindrical coordinates $\rho=(x^2+y^2)^{1/2}$, $\phi=\tan^{-1}(y/x)$, and $z$, with corresponding unit vectors $\hat{\boldsymbol{\rho}}=\hat{\mathbf{x}}\cos\phi+\hat{\mathbf{y}}\sin\phi$, $\hat{\boldsymbol{\phi}}=\hat{\mathbf{y}}\cos\phi-\hat{\mathbf{x}}\sin\phi$, and $\hat{\mathbf{z}}$.

Starting with a zero-field-cooled disk containing no vortices, application of a weak applied magnetic field $\mathbf{H}_a=H_a\hat{\mathbf{z}}$ simply induces azimuthal screening supercurrents in the disk. If the local magnetic field at the edge of the disk is less than the lower critical field $H_{c1}$, then no vortices penetrate into the sample. Because of strong demagnetizing effects, the net magnetic field bends around the sample, and screening currents, arising from the discontinuity of the radial magnetic field $H_\rho(\rho,z)$ at $z=\pm d/2$, flow over the entire surface of the disk. It can be shown[4,9,10] that in an applied magnetic field $\mathbf{H}_a=H_a\hat{\mathbf{z}}$ the induced current density, averaged over the film thickness, is

 

$$J_\phi(\rho)=-(4H_a/\pi d)\rho/(R^2-\rho^2)^{1/2} . \quad (1)$$

This expression applies for all $\rho<R$ except within a narrow region of negligible width $d$ or $\lambda$ (or $\Lambda$) at the film's edge.

The flux density $B_z(\rho,z=0)$ in the plane of the film can be calculated from the Biot-Savart law expressed as[4]

$$B_z(\rho,0)=B_a+\frac{\mu_0 d}{2\pi}\int_0^R G(\rho,\rho')J_\phi(\rho')d\rho' , \quad (2)$$

where $B_a=\mu_0 H_a$,

$$G(\rho,\rho')=K[k(\rho,\rho')]/(\rho+\rho')-E[k(\rho,\rho')]/(\rho-\rho') , \quad (3)$$

$$k(\rho,\rho')=2(\rho\rho')^{1/2}/(\rho+\rho') , \quad (4)$$

and $K$ and $E$ are complete elliptic integrals. It is found that $B_z(\rho,0)$ vanishes for $\rho<R$, and outside the film ($\rho>R$), $B_z(\rho,0)$ obeys[4]

$$B_z(\rho,0)=B_a\left\{1+\frac{2}{\pi}\left[\frac{1}{\sqrt{(\rho/R)^2-1}}-\sin^{-1}\left[\frac{R}{\rho}\right]\right]\right\} . \quad (5)$$

Strong demagnetizing effects are responsible for a sharp rise in the value of $B_z(\rho,0)$ near the film's edge. This inverse-square-root divergence is rounded off when one more carefully considers behavior on the small length scales $d$ and $\lambda$ (or $\Lambda$). For example, when $\lambda<d$, an analysis of demagnetization effects[11,12] yields $B_z(R,0)\approx(R/d)^{1/2}\mu_0 H_a$, aside from numerical factors of order unity.

When the applied field $H_a$ exceeds $(d/R)^{1/2}H_{c1}$, the local magnetic field at the film's edge exceeds $H_{c1}$, and (in the absence of surface-barrier effects) vortices then nucleate at the edge and penetrate into the superconductor. If there are pinning centers present, the distance to which the vortices penetrate depends upon the strength of vortex pinning in the film. According to the critical-state model,[13] in a quasisteady state the vortices penetrate only as far as necessary to reduce the magnitude of the local current density $\mathbf{J}$ to the level of the critical-current density $J_c$. In general, $J_c$ depends upon the local flux density $B$, but in this paper we neglect this dependence and consider only the Bean model,[6] which assumes a constant $J_c$. For simplicity we also ignore the effects of the reversible magnetization (i.e., we take $\mathbf{B}=\mu_0\mathbf{H}$ in the interior of the film), and we assume that there are no surface barriers to flux entry and exit. For the purposes of calculating critical-state profiles, these assumptions correspond to setting $H_{c1}=\Delta H_{\rm entry}=\Delta H_{\rm exit}=0$.[14-16]

As shown by Mikheenko and Kuzovlev,[4] the resulting current-density distribution $J_\phi(\rho)$ (again averaged over the film thickness) is

$$J_\phi(\rho)=-(2J_c/\pi)\tan^{-1}[(\rho/R)(R^2-a^2)^{1/2}/(a^2-\rho^2)^{1/2}], \quad \rho\le a , \quad (6a)$$

$$=-J_c, \quad a\le\rho<R . \quad (6b)$$

The magnitude of $J_\phi(\rho)$ is equal to $J_c$ throughout the annular vortex-filled region, whose inner radius $a$ is given by

$$a=R/\cosh(H_a/H_d) . \quad (7)$$

As pointed out by Norris,[1] the current density cannot change discontinuously in the interior of the film, and so the magnitude of $J_\phi(\rho)$ decreases continuously from $J_c$ at $\rho=a$, the outer radius of the vortex-free region, to zero at $\rho=0$, the center of the disk. Here

$$H_d=J_c d/2 \quad (8)$$

is a characteristic field for disk geometry; later we shall make use of the corresponding characteristic flux density $B_d=\mu_0 H_d=\mu_0 J_c d/2$. In the limit of small $H_a$ it can be shown from Eqs. (6) and (7) that $J_\phi(\rho)$ reduces to that given in Eq. (1). Shown in Fig. 1 are plots of $J_\phi(\rho)/J_c$ versus $\rho/R$. Note that these plots depend only upon the dimensionless ratio $x=H_a/H_d=B_a/B_d$.

The corresponding flux-density distribution $B_z(\rho,0)$ in the plane of the film can be calculated from Eq. (2) or, more conveniently, from the following expressions, which were derived using the weight-function approach of Ref. 4.

$$B_z(\rho,0)/B_d=0, \quad 0\le\rho\le a , \quad (9a)$$

$$=\cosh^{-1}(R/a)-\cosh^{-1}(R/\rho)+\int_{\sin^{-1}(a/\rho)}^{\pi/2}P_1(\rho/R,\theta)d\theta, \quad a\le\rho<R , \quad (9b)$$

$$=B_a/B_d+\int_{\sin^{-1}(a/R)}^{\pi/2}P_2(\rho/R,\theta)d\theta, \quad \rho>R , \quad (9c)$$

where

$$P_1(x,\theta)=\frac{2}{\pi}\left[\frac{(1-\theta\cot\theta)}{(1-x^2\sin\theta)^{1/2}}\right], \quad x<1 , \quad (10)$$

$$P_2(x,\theta)=\frac{2}{\pi}\left[\frac{1}{(x^2-\sin^2\theta)^{1/2}}-\frac{\sin^{-1}(x^{-1}\sin\theta)}{\sin\theta}\right], \quad x>1 . \quad (11)$$

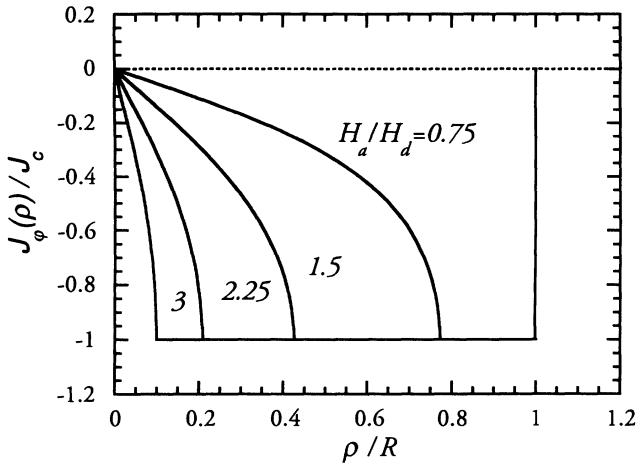


FIG. 1. Induced azimuthal current density $J_\phi(\rho)$, normalized to the critical-current density $J_c$, vs radius $\rho$ for thin-disk geometry in increasing magnetic field, calculated from Eq. (6) for normalized applied field values $H_a/H_d=B_a/B_d=0.75$, 1.50, 2.25, and 3.00, where $H_d=J_c d/2$. The vortex-free radius is $a=R/\cosh(H_a/H_d)$.

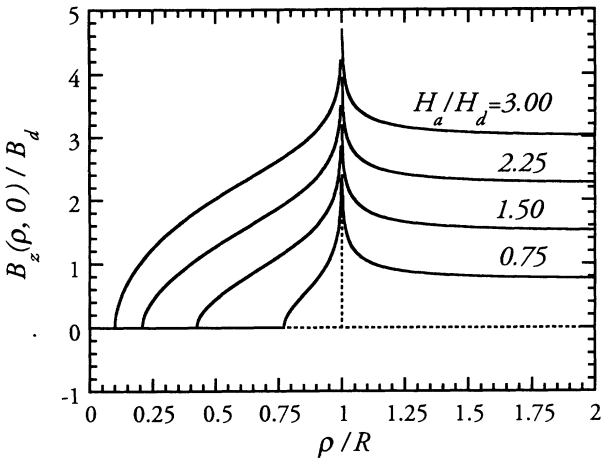


FIG. 2. Magnetic flux density in the film plane $B_z(\rho,0)$, normalized to $B_d=\mu_d H_d=\mu_0 J_c d/2$, vs radius $\rho$ for thin-disk geometry in increasing magnetic field, calculated from Eq. (9) for normalized applied field values $H_a/H_d=B_{al}/B_d=0.75$, 1.50, 2.25, and 3.00. The vortex-free radius is $a=R/\cosh(H_a/H_d)$.

Figure 2 shows plots of $B_z(\rho,0)/B_d$ versus $\rho/R$, corresponding to the current-density profiles in Fig. 1.

A striking result is that, according to Eq. (7), for finite applied fields $H_a$ the annular region where the current density is $J_c$ never fills the entire disk, and the critical-state flux-density profiles never penetrate all the way to the center, where $B_z(0,0)$ remains equal to zero. In practice, however, the above two-dimensional approach breaks down and $B_z(0,0)$ becomes nonzero when the vortex-free radius $a$ approaches the largest of the quantities $d$, $\lambda$, and $\Lambda$.[17]

Of interest for the computation of ac losses are the current-density and magnetic-field profiles produced when the applied field $H_a$ oscillates quasistatically between the values $+h_0$ and $-h_0$. We begin with a current-density profile with vortex-free radius now defined as $a=R/\cosh(h_0/H_d)$ corresponding to $H_a=h_0$, and we consider the changes that occur as $H_a$ is reduced from $+h_0$ to $-h_0$. As explained by Zhu *et al.*,[5] the resulting current-density profile must have $J_\phi(\rho)=+J_c$ within an annulus of inner and outer radii $b$ and $R$. The reason for this is that vortices near the outer radius must experience a Lorentz force that drives them out of the sample as the field is initially decreasing. This leads to a finite azimuthal electric field in the outer annulus, where the flux density is changing. In film geometry, the current density $J_\phi(\rho)$ cannot change discontinuously[1] from $-J_c$ to $+J_c$ but instead must be a continuous function of $\rho$. The appropriate solution is a superposition of a frozen-flux contribution given in Eq. (6) and a reverse-field contribution that is also obtained from Eq. (6), but with $J_c$ replaced by $-2J_c$ and $a$ replaced by $b$, where[5]

$$b=R/\cosh[(h_0-H_a)/2H_d] . \tag{12}$$

The reverse-field contribution leaves the previous flux-density distribution $B_z(\rho,0)$ unchanged for $\rho<b$, but assures that $J_\phi(\rho)=J_c$ in the outer annulus $\rho>b$, where vortices are moving out of the sample or antivortices are moving in. The resulting current-density distribution in the film is[5]

$$J_\phi(\rho)=-(2J_c/\pi)\tan^{-1}[(\rho,R)(R^2-a^2)^{1/2}/(a^2-\rho^2)^{1/2}]$$

$$+(4J_c/\pi)\tan^{-1}[(\rho/R)(R^2-b^2)^{1/2}/(b^2-\rho^2)^{1/2}],\quad \rho\le a , \tag{13a}$$

$$=-J_c+(4J_c/\pi)\tan^{-1}[(\rho/R)(R^2-b^2)^{1/2}/(b^2-\rho^2)^{1/2}],\quad a\le\rho\le b , \tag{13b}$$

$$=+J_c,\quad b\le\rho<R . \tag{13c}$$

Shown in Fig. 3 are plots of the normalized current density $J_\phi(\rho)/J_c$ versus $\rho/R$ as the applied field $H_a$ is reduced from $+h_0$ to $-h_0$. These plots depend only upon the dimensionless ratio $x=H_a/H_d=B_a/B_d$. Figure 4 shows corresponding plots of the normalized flux density in the film plane $B_z(\rho,0)/B_d$ versus $\rho/R$. These are calculated numerically from the following expressions, which are derived by superposition from Eq. (9):

$$B_z(\rho,0)/B_d=0, \quad 0\le\rho\le a\le b\le R \ , \tag{14a}$$

$$=[\cosh^{-1}(R/a)-\cosh^{-1}(R/\rho)]+\int_{\sin^{-1}(a/\rho)}^{\pi/2}P_1(\rho/R,\theta)d\theta, \quad a\le\rho\le b\le R \ , \tag{14b}$$

$$=[\cosh^{-1}(R/a)-\cosh^{-1}(R/\rho)]-2[\cosh^{-1}(R/b)-\cosh^{-1}(R/\rho)]$$
$$+\int_{\sin^{-1}(a/\rho)}^{\sin^{-1}(b/\rho)}P_1(\rho/R,\theta)d\theta-\int_{\sin^{-1}(b/\rho)}^{\pi/2}P_1(\rho/R,\theta)d\theta, \quad a\le b\le\rho<R \ , \tag{14c}$$

$$=B_a/B_d+\int_{\sin^{-1}(a/R)}^{\sin^{-1}(b/R)}P_2(\rho/R,\theta)d\theta-\int_{\sin^{-1}(b/R)}^{\pi/2}P_2(\rho/R,\theta)d\theta, \quad a\le b\le R<\rho \ . \tag{14d}$$

As expected, the profile of $B_z(\rho,0)$ versus $\rho$ when $H_a=-h_0$ is the negative of that when $H_a=+h_0$. As will be shown in Sec. III, this leads to hysteretic magnetization curves that are symmetric with respect to the origin.

The current-density and flux-density profiles produced when the applied field $H_a$ increases from $-h_0$ to $+h_0$ are simply mirror images of those shown in Figs. 3 and 4. They are given as the superposition of a frozen-flux contribution calculated from Eq. (6), but with $J_c$ replaced by $-J_c$ and a reverse-field contribution also calculated from Eq. (6), but with $J_c$ replaced by $2J_c$ and $a$ replaced by $b$, where[5]

$$b=R/\cosh[(h_0+H_a)/2H_d] \ . \tag{15}$$

## III. MAGNETIZATION HYSTERESIS IN A THIN SUPERCONDUCTING DISK

The magnetic moment of a disk in a perpendicular magnetic field has only a $z$ component, which can be calculated from the current density $J_\phi(\rho)$ using[18]

$$m_z=\pi d\int_0^R\rho^2J_\phi(\rho)d\rho \ , \tag{16}$$

and the magnetization can be calculated from $M_z=m_z/V$, where $V=\pi R^2d$ is the sample volume.

When a small alternating field $H_a$ is applied, then, assuming no vortex penetration, the screening is maximum, and the magnetization calculated from Eqs. (1) and (16) is

$$M_z=-\chi_0H_a \ , \tag{17}$$

where $\chi_0=8R/3\pi d$. Thus the external magnetic susceptibility[11] in this case of perfect screening is $\chi=-\chi_0$.

Starting from the zero-field-cooled state, and applying a magnetic field $H_a$ that causes an annulus of vortex penetration to occur, leads to a magnetization whose magnitude is less than that given in Eq. (17). Substitution of the current distribution of Eq. (6) into Eq. (16) yields the initial magnetization

$$M_z=-\chi_0H_aS(H_a/H_d) \ , \tag{18}$$

where[4]

$$S(x)=\frac{1}{2x}\left[\cos^{-1}\left[\frac{1}{\cosh x}\right]+\frac{\sinh x}{\cosh^2x}\right] \ . \tag{19}$$

The function $S(x)$ is a monotonically decreasing function of $x$, behaving as $S(x)\approx1-x^2/2$ for $x\ll1$ and

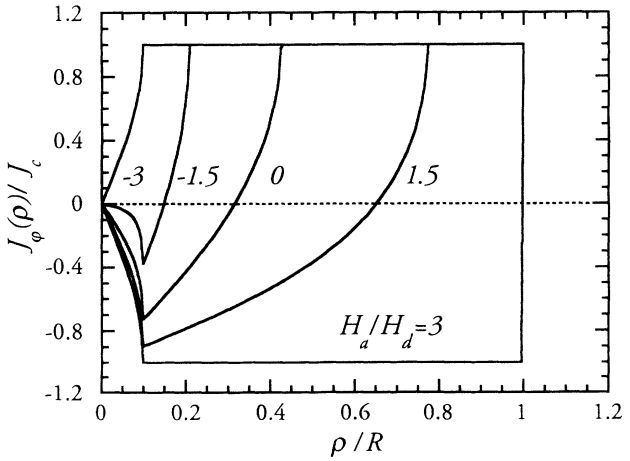


FIG. 3. Azimuthal current density $J_\phi(\rho)$ [Eq. (13)], normalized to the critical-current density $J_c$, vs radius $\rho$ for thin-disk geometry as the applied magnetic field $H_a$ is reduced from $h_0=3H_d$ to $-h_0$ (normalized applied fields $H_a/H_d=B_a/B_d=3.0$, 1.5, 0.0, $-1.5$, and $-3.0$), where $H_d=J_cd/2$. The vortex-free radius is $a=R/\cosh(h_0/H_d)$. The inner radius of the annulus where $J_\phi(\rho)=J_c$ and the flux density is decreasing is $b=R/\cosh[(h_0-H_a)/2H_d]$.

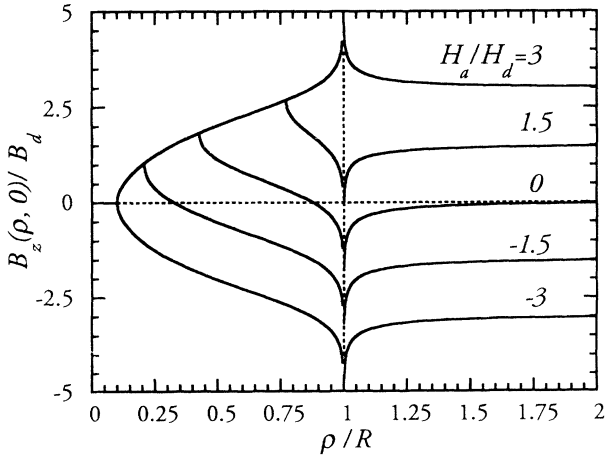


FIG. 4. Magnetic flux density in the film plane $B_z(\rho,0)$ [Eq. (14)], normalized to $B_d=\mu_0H_d=\mu_0J_cd/2$, vs radius $\rho$ for thin-disk geometry as the applied magnetic field $H_a$ is reduced from $h_0=3H_d$ to $-h_0$ (normalized applied fields $H_a/H_d=B_a/B_d=3.0$, 1.5, 0.0, $-1.5$, and $-3.0$). The vortex-free radius is $a=R/\cosh(h_0/H_d)$. The inner radius of the annulus where $J_\phi(\rho)=J_c$ and the flux density is decreasing is $b=R/\cosh[(h_0-H_d)/2H_d]$.

$S(x)\approx\pi/4x$ for $x\gg1$. For $H_a/H_d\ll1$, Eq. (18) reduces to Eq. (17), while for $H_a/H_d\gg1$ the magnetization approaches the saturation value $M_z=-M_{\rm sat}$, where $M_{\rm sat}=(\pi\chi_0/4)H_d=J_cR/3$ corresponds to the result obtained from Eq. (16) when $J_\phi(\rho)=J_c$. Because of Eq. (7), however, complete saturation never occurs for a finite applied field; in this two-dimensional approach, as discussed in Sec. II, the zone where the current density is $J_c$ never penetrates all the way to the center. The initial magnetization given by Eq. (18) is shown as the dashed curve in Fig. 5.

If the applied magnetic field $H_a$ oscillates quasistatically between $+h_0$ and $-h_0$, the current distribution of Eq. (13) yields the magnetization[5]

$$M_{\downarrow z}=-\chi_0h_0S(h_0/H_d)+\chi_0(h_0-H_a)S[(h_0-H_a)/2H_d)]\ , \tag{20}$$

when $H_a$ is decreasing from $+h_0$ to $-h_0$ [see Eq. (12)]. Similarly, the magnetization is[5]

$$M_{\uparrow z}=+\chi_0h_0S(h_0/H_d)-\chi_0(h_0+H_a)S[(h_0+H_a)/2H_d)]\ , \tag{21}$$

when $H_a$ is increasing from $-h_0$ to $+h_0$ [see Eq. (15)]. The solid curves shown in Fig. 5 are magnetization hysteresis loops calculated from Eqs. (20) and (21).

## IV. GENERAL RELATIONS BETWEEN ac LOSSES AND SUSCEPTIBILITY IN A THIN SUPERCONDUCTING DISK

When the time dependence of the magnetic moment $m_z(t)$ or the magnetization $M_z(t)$ of the sample is known,

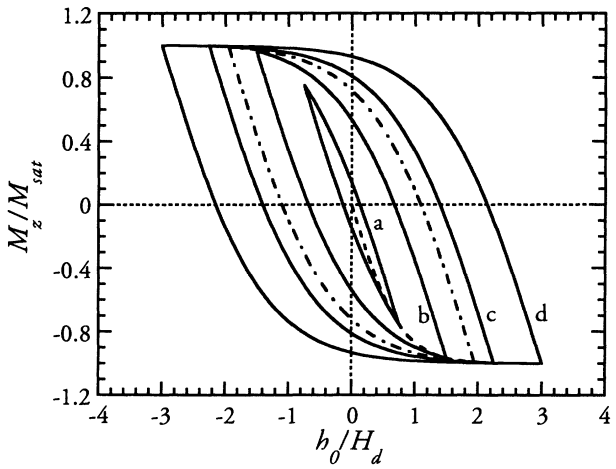


FIG. 5. Magnetization $M_z$ vs applied field $H_a$. The dashed curve shows the initial magnetization [Eq. (18)], starting from the zero-field-cooled state, while the solid curves show magnetization hysteresis loops when $H_a$ is cycled between $+h_0$ to $-h_0$ [Eqs. (20) and (21)] [normalized fields $h_0/H_d$=(a) 0.75, (b) 1.50, (c) 2.25, and (d) 3.00]. $M_z$ is normalized to the saturation magnetization $M_{\rm sat}=(\pi\chi_0/4)H_d=J_cR/3$, while $H_a$ is normalized to $H_d=J_cd/2$. The dot-dashed curves show the magnetization hysteresis at the special value of $x=h_0/H_d=1.942$, where $\chi''=A/\pi h_0^2$ has its maximum value $0.241\chi_0$.

so also is the time dependence of the magnetic flux through the circuit that produces the applied magnetic field $\mathbf{H}_a(t)=H_a\hat{\mathbf{z}}(t)$. When $H_a$ oscillates between $+h_0$ and $-h_0$ with period $T$, we may obtain the sample's ac loss per cycle by integrating the power $P=IV$ delivered to the magnet that produces $H_a$. The resulting energy dissipation per cycle per unit volume of sample is

$$W_V=\mu_0\int_0^T H_a(t)\frac{dM_z(t)}{dt}dt\ . \tag{22}$$

If $H_a(t)=h_0\cos\omega t$, where $\omega=2\pi/T$, the magnetization $M_z(t)$ also is periodic with period $T$, and it is convenient to Fourier analyze it as follows:

$$M_z(t)=\sum_{n=1}^{\infty}(\chi_n'\cos n\omega t+\chi_n''\sin n\omega t)h_0\ , \tag{23}$$

where the ac susceptibility coefficients $\chi_n'$ and $\chi_n''$ are obtained from

$$\chi_n'=\frac{\omega}{\pi h_0}\int_0^T M_z(t)\cos n\omega t dt\ , \tag{24}$$

$$\chi_n''=\frac{\omega}{\pi h_0}\int_0^T M_z(t)\sin n\omega t dt\ . \tag{25}$$

Often the response of the sample is measured only at the fundamental frequency ($n=1$), such that only the values of $\chi'=\chi_1'$ and $\chi''=\chi_1''$ are obtained. In this case $\chi'$ and $\chi''$ can be thought of as the real and imaginary parts of the complex susceptibility $\tilde{\chi}=\chi'+i\chi''$. That is, if $\tilde{H}_a=h_0\exp(-i\omega t)$, then the $n=1$ part of the magnetization [Eq. (23)] is $M_{1z}=\mathrm{Re}\tilde{M}_{1z}$, where $\tilde{M}_{1z}=\tilde{\chi}\tilde{H}_a$. The real part of $\tilde{\chi}$ ($\chi'$) measures the inductive response, while the imaginary part ($\chi''$) measures the resistive response. To see the connection between $\chi''$ and the hysteretic ac losses, note that when Eq. (23) is substituted into Eq. (22) and the integration is carried out, only the $n=1$ term involving $\chi''=\chi_1'$ suvives, and the result may be written as

$$W_V=\mu_0\oint H_a dM_z=\mu_0A\ , \tag{26}$$

where

$$\chi''=\chi_1''=A/\pi h_0^2\ . \tag{27}$$

Thus $\chi''=\chi_1''$ has a simple geometric interpretation as the ratio of the area $A=\oint H_a dM_z=\oint M_z dH_a$ of the magnetization hysteresis loop to the area $\pi h_0^2$ of a circle whose radius is the ac field amplitude $h_0$. Exactly the same interpretation can be given to $\chi''$ for an infinitely long cylinder in a parallel applied magnetic field.[16] We emphasize that our definition of $\tilde{\chi}$ corresponds to the external susceptibility discussed in Ref. 11, and not to the internal susceptibility.

## V. CALCULATIONS OF THE ac LOSSES AND SUSCEPTIBILITY IN A THIN SUPERCONDUCTING DISK FOR CONSTANT $J_c$

When the critical-current density $J_c$ is independent of field, the hysteretic magnetization in an applied ac field of amplitude $h_0$ is given by Eqs. (20) and (21). Substitution

of these into Eqs. (24) and (25) for odd $n$ yields

$$\chi_n'=\frac{2\chi_0}{\pi}\int_0^{\pi}(1-\cos\theta)S[(x/2)(1-\cos\theta)]\cos n\theta d\theta\ , \tag{28}$$

$$\chi_n''=\frac{2\chi_0}{\pi}\int_0^{\pi}\{-S(x)+(1-\cos\theta)S[(x/2)(1-\cos\theta)]\}\sin n\theta d\theta\ , \tag{29}$$

where $x=h_0/H_d$, $H_d=J_c d/2$, and $\chi_0=8R/3\pi d$. Because of the symmetry of the magnetization curves $[M_{\uparrow z}(-H_a)=-M_{\downarrow z}(H_a)]$, we find $\chi_n'=\chi_n''=0$ for all even $n$. The expression for $\chi_1'$ agrees with Eq. (21) of Ref. 5, except for the different definition of magnetic susceptibility.

The $n=1$ components of the ac susceptibility can be shown to have the limiting behavior

$$\chi'\approx-\chi_0(1-\tfrac{15}{32}x^2),\quad x\ll 1\ , \tag{30}$$

$$\chi''\approx\chi_0 x^2/\pi,\quad x\ll 1\ , \tag{31}$$

$$\chi'\approx-\chi_0(1.330x^{-3/2}-0.634x^{-5/2}),\quad x\gg 1\ , \tag{32}$$

$$\chi''\approx\chi_0(x^{-1}-1.059x^{-2}),\quad x\gg 1\ . \tag{33}$$

We also find from numerical calculations that the peak in $\chi''$ occurs at $x=1.942$, where $\chi''=\chi''_{\max}=0.241\chi_0$ and $\chi'=-0.382\chi_0$.

Since $x=h_0/H_d$, Eq. (32) shows that the magnitude of $\chi'$ varies as $h_0^{-3/2}$ for large $h_0$, in agreement with an assertion by Mikheenko and Kuzovlev,[4] but we agree with Zhu *et al.*[5] that the expression for $\chi'$ in Ref. 4 is quantitatively incorrect. On the other hand, Eq. (32) contradicts the claim of Zhu *et al.*[5] that the magnitude of $\chi'$ varies as $h_0^{-1}$ for large $h_0$.

Figure 6 shows plots of both $\chi'$ and $\chi''$ versus $x=h_0/H_d$, and Fig. 7 shows a log-log plot of $\chi''$ versus $x$.

The nonlinear response of the superconductor when pinning is present is reflected in the presence of higher harmonics in the voltage wave form and the appearance of susceptibility components with $n=3$, 5, etc. For linear response, only the fundamental ($n=1$) components would be present, as is the case for eddy current damping in a normal-conducting disk. Despite the nonlinearity, all the even harmonics are zero because of the symmetry of the magnetization hysteresis curves. Shown in Fig. 8 are the components $\chi_3'$ and $\chi_3''$, while Fig. 9 displays the components $\chi_5'$ and $\chi_5''$. Note that, for finite $h_0/H_d$, $\chi_1'$ (Fig. 6) is never zero, while $\chi_3'$ (Fig. 8) has one zero and $\chi_5'$ (Fig. 9) two zeros. Also note that, while $\chi_3''$ and $\chi_5''$ have a similar appearance, except for a difference in amplitude by a factor of about 5, $\chi_5''$ has an extra wiggle near $h_0/H_d=1$.

## VI. DISCUSSION OF RESULTS

In this paper we have combined the approaches of Mikheenko and Kuzovlev[4] and Zhu *et al.*[5] to calculate the critical-state behavior of the current density and flux density, the ac-susceptibility components, and the hysteretic ac losses for a thin superconducting disk of thickness $d$ and radius $R$. Our expression for $\chi'$ [Eq. (28)] agrees with that in Ref. 5, except that the authors used a different definition for the magnetic susceptibility. As was shown in Ref. 5, the calculation of the ac susceptibility given in Ref. 4 is incorrect.

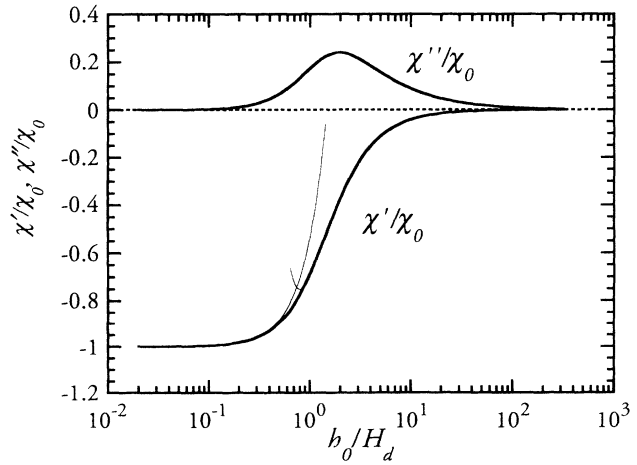


FIG. 6. Real ($\chi'$) and imaginary ($\chi''$) parts of the $n=1$ (fundamental-frequency) complex susceptibility, normalized to $\chi_0=8R/3\pi d$, as a function of $h_0/H_d$, where $h_0$ is the ac amplitude and $H_d=J_c d/2$. The thick curves are calculated from Eqs. (28) and (29), and the thin curves show the limiting expressions for $\chi'$ given in Eqs. (30) and (32).

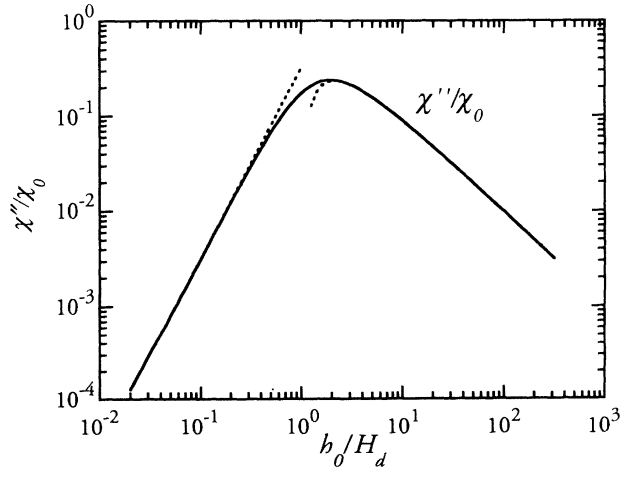


FIG. 7. Imaginary part $\chi''$ of the $n=1$ (fundamental-frequency) complex susceptibility, normalized to $\chi_0=8R/3\pi d$, as a function of $h_0/H_d$, where $h_0$ is the ac amplitude and $H_d=J_c d/2$. The solid curve is calculated from Eq. (29), and the dashed curves show the limiting expressions for $\chi''$ given in Eqs. (31) and (33). The ac loss per cycle per unit volume is $\mu_0\chi''\pi h_0^2$.

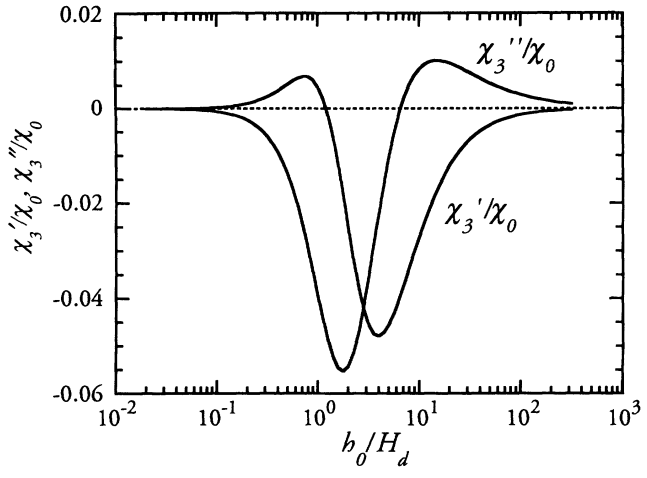


FIG. 8. Real ($\chi_3'$) and imaginary ($\chi_3''$) parts of the $n=3$ (third-harmonic) complex susceptibility, normalized to $\chi_0=8R/3\pi d$, as a function of $h_0/H_d$, where $h_0$ is the ac amplitude and $H_d=J_c d/2$. The solid curves are calculated from Eqs. (28) and (29).

Previous calculations of the magnetic susceptibility have been presented in Refs. 17 and 19. A key assumption made in both papers, however, is that the current density **J** in the film always has magnitude $J_c$ in the flux-penetrated regions, and that it reverses direction and thus changes discontinuously at the inner radius of the advancing flux front. While this assumption is valid in the critical-state model for an infinite slab or cylinder in a parallel magnetic field, it is not correct for the case of film geometry, as shown explicitly in Fig. 3. Thus, while the results of Refs. 17 and 19 evidently give a reasonable approximation to the behavior of $\chi'$ and $\chi''$ versus $x=h_0/H_d$, they cannot give a quantitatively correct description of the ac susceptibility.

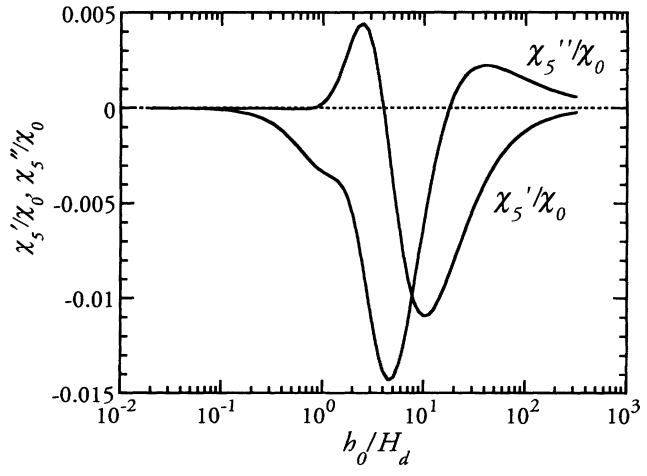


FIG. 9. Real ($\chi_5'$) and imaginary ($\chi_5''$) parts of the $n=5$ (fifth-harmonic) complex susceptibility, normalized to $\chi_0=8R/3\pi d$, as a function of $h_0/H_d$, where $h_0$ is the ac amplitude and $H_d=J_c d/2$. The solid curves are calculated from Eqs. (28) and (29).

Related work also has been done recently by Brandt, Indenbom, and Forkl,[2] who applied the Norris approach[1] to obtain the hysteresis losses of a long, thin strip of length $L$, width $2a$, and thickness $d$ in the presence of an oscillating applied magnetic field of frequency $\nu$ and amplitude $h_0$. They correctly included the effects of screening currents that flow below the critical value in the frozen-flux portions of the strip, and they accounted for the fact that the current density cannot change discontinuously in a thin film. They found that the rate of energy dissipation is

$$P=4\nu\mu_0 a^2 dL\, J_c h_0[(2/x)\ln\cosh x-\tanh x]\,, \tag{34}$$

where $x=h_0/H_f$ and $H_f=J_c d/\pi$. For $h_0\ll H_f$ this gives $P=(2\pi\nu\mu_0 a^2 L/3H_f^2)h_0^4$, and for $h_0\gg H_f$, $P=4\nu\mu_0 a^2 dLJ_c(h_0-1.386H_f)$.

Our corresponding results for a disk of radius $R$ and thickness $d$ are

$$P=\pi^2\nu\mu_0 R^2 dh_0^2\chi''(x)\,, \tag{35}$$

where $x=h_0/H_d$ and $H_d=J_c d/2$. For $h_0\ll H_d$ this gives [Eq. (31)] $P=(8\nu\mu_0 R^3/3H_d^2)h_0^4$, and for $h_0\gg H_d$ [Eq. (33)], $P=(4\pi\nu\mu_0 R^3 dJ_c/3)(h_0-1.059H_d)$. As expected, the power-law dependence of $P$ upon $h_0$ is the same in the two limits; i.e., $P\propto h_0^4$ for small $h_0$ and $P\propto h_0$ for large $h_0$ for both strips and disks. Recent work by other authors[3] has shown that in the critical state the behavior of thin-film strips is similar in many respects to that of thin-film disks.

The behavior of a thin film in a perpendicular field is very different, however, from the critical-state behavior of an infinite slab or cylinder in a time-varying parallel magnetic field.[13] For example, in a slab of thickness $2W$, the field $H^*$ that pushes a flux front (in which the magnitude of the current denisty is $J_c$) to the center is given by $H^*=J_c W$. (Here it is assumed that $B\gg H_{c1}$.) The saturation magnetization is then $M_{\rm sat}=J_c W/2$, so that $M_{\rm sat}/H^*=\frac{1}{2}$. In a film of radius $R$ and thickness $d$, however, we find that the saturation magnetization is $M_{\rm sat}=J_c R/3$, while the characteristic applied field at which the flux front is pushed a significant distance in toward the center is $H_d=J_c d/2$. Thus $M_{\rm sat}/H_d=2R/3d\gg 1$. Another important difference is that $M_z$ saturates at exactly $H^*$ for the slab, while saturation occurs only in infinite applied field for the disk [see Eq. (7)].

What is common to the hysteretic critical-state behavior of both thin films and slabs is that during quasistatic changes of an applied magnetic field, vortices move (and the local flux density **B** changes) wherever the magnitude of the current density **J** (assumed perpendicular to the vortices) exceeds the critical value $J_c$. What is different about the two geometries is that in the slab the local current density **J** can change only where the flux density **B** changes. In a film, on the other hand, changes in the applied field induce screening currents **J** (associated with the discontinuity in the changing *tangential* component of the magnetic field at the top and bottom of the film) to flow not just at the edges but throughout the film. However, these currents do not cause flux motion or a

change in the *perpendicular* component of the magnetic flux density unless the magnitude of **J** exceeds $J_c$.

The results given in this paper are restricted to slow, quasistatic flux changes for which the magnitude of the electric field **E** induced by the moving magnetic flux is small by comparison with $\rho_f J_c$, where $\rho_f$ is the flux-flow resistivity. Under these conditions, the magnitude of the induced current density **J** is always very close to the critical current density $J_c$ in regions of the sample where $B_z$ is changing. Rapid variation of the externally applied field, on the other hand, causes rapid flux motion, generates large values of the magnitude of **E** (exceeding $\rho_f J_c$), and induces current densities of magnitude well in excess of $J_c$. Such a high-frequency response of a thin disk requires a different approach, accounting for flux-flow eddy-current losses, such as those presented in Refs. 20 and 21.

In summary, we have extended the results of Mikheenko and Kuzovlev,[4] as amended by Zhu *et al.*,[5] to calculate the critical-state current-density and flux-density profiles in a thin superconducting disk subjected to a slowly varying perpendicular applied field. We in turn used these results to calculate the magnetization hysteresis, ac losses, and nonvanishing ac-susceptibility components $\chi_n'$ and $\chi_n''$, where $n$ is odd. We also pointed out how the current and field penetration, magnetization, and energy dissipation for a film in a perpendicular field differ from those for a slab or cylinder in a parallel field.

## ACKNOWLEDGMENTS

We thank M. R. Beasley and the Department of Applied Physics for their hospitality at Stanford University, where this work was performed. We also thank E. H. Brandt, J. Lockhart, M. McElfresh, E. Zeldov, and J. Zhu for helpful discussions and correspondence. Ames Laboratory is operated for the U.S. Department of Energy by Iowa State Univesity under Contract No. W-7405-Eng-82. This research was supported by the Director for Energy Research, Office of Basic Energy Sciences, by the Midwest Superconductivity Consortium through D.O.E. grant. No. DE-FG02-90ER45427, by the Electric Power Research Institute, by the Spanish CICYT project MAT91-0955, and by CIRIT.

[1]W. T. Norris, J. Phys. D **3**, 489 (1970).

[2]E. H. Brandt, M. Indenbom, and A. Forkl, Europhys. Lett. **22**, 735 (1993).

[3]M. Darwin, J. Deak, L. Hou, M. McElfresh, E. Zeldov, J. R. Clem, and M. Indenbom, Phys. Rev. B **48**, 13 192 (1993).

[4]P. N. Mikheenko and Yu. E. Kuzovlev, Physica C **204**, 229 (1993).

[5]J. Zhu, J. Mester, J. Lockhart, and J. Turneaure, Physica C **212**, 216 (1993).

[6]C. P. Bean, Phys. Rev. Lett. **8**, 250 (1962).

[7]J. Pearl, in *Proceedings of the Ninth International Conference on Low Temperature Physics,* edited by J. G. Daunt, D. V. Edwards, F. J. Milford, and M. Yaqub (Plenum, New York, 1965), Part A, p. 566; J. Pearl, Appl. Phys. Lett. **5**, 65 (1964).

[8]P. G. deGennes, *Superconductivity of Metals and Alloys* (Benjamin, New York, 1966).

[9]L. D. Landau and E. M. Lifshitz, *Theoretical Physics,* Vol. 8, *Electrodynamics of Continuous Media* (Nauka, Moscow, 1982).

[10]M. B. Ketchen, W. J. Gallagher, A. W. Kleinsasser, S. Murphy, and J. R. Clem, in *SQUID '85–Superconducting Quantum Interference Devices and Their Applications,* edited by H. D. Hahlbohm and H. Lübbig (de Gruyter, Berlin, 1985), p. 865.

[11]R. B. Goldfarb, M. Lelental, and C. A. Thompson, in *Magnetic Susceptibility of Superconductors and Other Spin Systems,* edited by R. A. Hein, T. L. Francavilla, and D. H. Liebenberg (Plenum, New York, 1992), p. 49.

[12]E. Zeldov, J. R. Clem, M. McElfresh, and M. Darwin, Phys. Rev. B **49**, 9802 (1994).

[13]A. M. Campbell and J. E. Evetts, Adv. Phys. **21**, 199 (1972).

[14]J. R. Clem, J. Appl. Phys. **50**, 3518 (1979).

[15]D.-X. Chen and A. Sanchez, Phys. Rev. B **45**, 10793 (1992).

[16]J. R. Clem, in *Magnetic Susceptibility of Superconductors and Other Spin Systems* (Ref. 11), p. 177.

[17]J. Z. Sun, M. J. Scharen, L. C. Bourne, and J. R. Schrieffer, Phys. Rev. B **44**, 5275 (1991).

[18]J. D. Jackson, *Classical Electrodynamics* (Wiley, New York, 1962), p. 146.

[19]V. A. Atsarkin, G. A. Vasneva, and N. E. Noginova, *Superconductivity* **5**, 417 (1992).

[20]E. H. Brandt, Phys. Rev. Lett. **71**, 2642 (1993).

[21]E. H. Brandt, Phys. Rev. B **49**, 9024 (1994).